16èmes Journées de l'Hydrodynamique

27-29 novembre 2018 - Marseille

ETUDE EXPERIMENTALE DES EFFETS DU SILLAGE D'UN LARGE OBSTACLE POSE SUR LE COMPORTEMENT D'UNE HYDROLIENNE

EXPERIMENTAL STUDY OF THE WAKE OF A WIDE WALL-MOUNTED OBSTACLE ON THE BEHAVIOUR OF A MARINE CURRENT TURBINE

Benoît GAURIER[1], Maria IKHENNICHEU[1], Philippe DRUAULT[2], Grégory GERMAIN[1], Jean-Valéry FACQ[1], Grégory PINON[3]

[1]Ifremer, Metocean Laboratory, 150 Quai Gambetta 62200 Boulogne sur Mer, France.
benoit.gaurier@ifremer.fr
[2]Sorbonne Université, UPMC Univ Paris 06, CNRS, UMR 7190, Institut Jean Le Rond d'Alembert, 75005 Paris, France
philippe.druault@sorbonne-universite.fr
[3]LOMC - UMR 6295, Normandie Univ, UNIHAVRE, CNRS, 76600 Le Havre.
gregory.pinon@univ-lehavre.fr

Résumé

Dans les zones à forts courants telles que celles adaptées à l'exploitation des énergies marines renouvelables, les variations de bathymétrie créent de fortes fluctuations de vitesse. Des expériences ont montré que de larges obstacles cylindriques généraient de fortes fluctuations de vitesses, telles que celles observables en mer. Afin d'étudier les effets de ces fluctuations de chargement sur le comportement d'une hydrolienne, un dispositif expérimental a été développé dans le bassin à circulation de l'Ifremer à Boulogne-sur-mer, en positionnant un cylindre et une turbine dans son sillage. Des mesures PIV simultanées donnent accès à la vitesse du fluide en amont de la turbine. La vitesse et les efforts sont comparés en terme de corrélation croisées, de cohérence et leur contenu spectral est étudié. Les résultats montrent que les efforts suivent les fluctuations de vitesses jusqu'à une fréquence de $1H_z$ et les fluctuations de vitesse à basse fréquence ont plus d'impact lorsque la turbine est en fonctionnement. La cohérence entre la vitesse du fluide et la vitesse de rotation diffère de celle des chargements, probablement dû au système de contrôle de rotation de la machine.

Summary

In high flow velocity areas like those suitable for marine energy application, bathymetry variations create strong velocity fluctuations in the water column. Experiments showed

that wide cylindrical obstacles generate large velocity fluctuations, like those measured at sea. In order to study the effects of these fluctuations on the turbine behaviour, an experimental set-up has been developed in the circulating tank of Ifremer in Boulogne-sur-mer by positioning a cylinder and a turbine in its wake. Simultaneous PIV measurements give access to the flow velocity upstream of the turbine. Velocity and efforts are compared in terms of cross-correlation, coherence and their spectral content is studied. Results show that the turbine loads follow velocity fluctuations until a frequency of $1H_z$ and that low frequency velocity fluctuations have an higher impact when the turbine is in function. Coherence between fluid velocity and the rotation speed differs from coherence to the loads, probably due to the rotation control system.

I – Introduction

For the past ten years, high level of turbulence have been measured in tidal stream sites [9]. In France, the Alderney Race (Raz-Blanchard) is one of the most energetic location with a high turbulence rate in the entire water column, originating mainly from large bathymetry variations (figure 1). This turbulence can affect significantly the performance and fatigue of tidal turbines [1, 7]. Figure 1b illustrates bathymetry variations profiles in the area of interest for tidal turbine application, with a mean variation of $5m$ and large elevation exceeding $10m$, in profile 2 in particular. These elevations can be experimentally represented by a unitary wall-mounted obstacle. Recent experiments [5] showed that an isolated large aspect ratio wall-mounted square cylinder produces a very extended wake, with large velocity fluctuations. In some cases, large coherent energetic structures, able to rise up to the surface, are produced with a potential impact on tidal turbines, present in the wake of the obstacles.

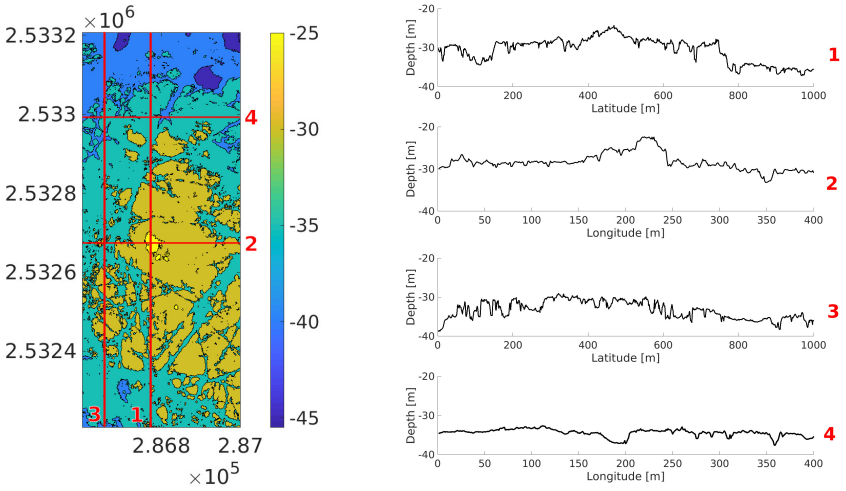

(a) Depth $[m]$ in a $400 \times 1000m^2$ area of interest

(b) Bottom elevation profiles

Figure 1 – Bathymetry of the Alderney Race (Raz-Blanchard), from [8]

The effect of the velocity fluctuations induced by a wide wall-mounted obstacle on the behaviour of a marine current turbine model will be investigated here. First, the experimental set up is described, then the results obtained are presented and finally a conclusion is proposed.

II – Experimental Set-up

Tests have been carried out in the wave and current circulating tank of IFREMER located in Boulogne-sur-Mer (France), presented in figure 2. The test section is $18m$ long, $4m$ wide and $2m$ deep. The incoming flow is assumed to be steady and constant. By means of a grid combined with a honeycomb, that acts as a flow straightener, placed at the inlet of the working section, a low turbulent intensity of $I_\infty = 1.5\%$ is achieved.

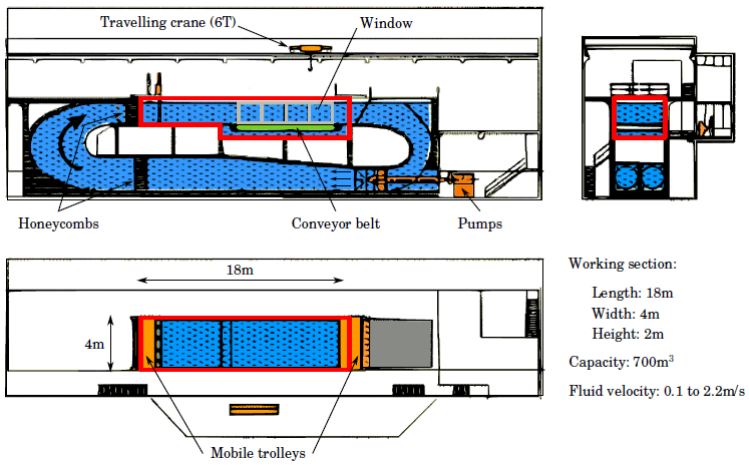

Figure 2 – IFREMER Flume tank in Boulogne-sur-Mer

The three instantaneous velocity components are denoted (u, v, w) along the (x, y, z) directions respectively. Each instantaneous velocity component is separated into a mean value and a fluctuation part, according to the Reynolds decomposition: $u(t) = \overline{u} + u'(t)$, where an overbar indicates the time average. Turbulence intensity I_∞ in the incoming flow is defined by the classical equation 1, where σ stands for the standard-deviation.

$$I_\infty = 100\sqrt{\frac{\frac{1}{3}[\sigma(u)^2 + \sigma(v)^2 + \sigma(w)^2]}{\overline{u}^2 + \overline{v}^2 + \overline{w}^2}} \tag{1}$$

In the following, non dimensional lengths are used for all parameters indexed by *: $x^* = x/H$ for instance, with $H = 0.25m$ the obstacle height. At the upstream obstacle position, the boundary layer height δ^* is calculated with equation 2, with U_∞ the far upstream velocity.

$$\delta^* = \delta^*_{95} = z^*(\overline{u} = 0.95 \times U_\infty) = 1.3 \tag{2}$$

In order to consider turbulent event interaction with the free surface, experiments are achieved in Froude (F_r) similitude (see equation 3). Furthermore, Reynolds number R_e must be as high as achievable to be closer to real conditions.

$$F_r = \frac{U_\infty}{\sqrt{gd}} \quad \text{and} \quad R_e = \frac{HU_\infty}{\nu} \tag{3}$$

Finally, all the experimental parameters are given in table 1, with d the water depth.

	Scale	U_∞ $[m/s]$	H $[m]$	d $[m]$	R_e	F_r
Alderney Race	1	5	5	40	2.5×10^7	0.25
Flume tank	1/20	1	0.25	2	2.5×10^5	0.23

Table 1 – *in situ* and experimental conditions

Previous studies showed that, with a wide wall-mounted cylinder in the tank, large velocity fluctuations associated with high intensity turbulent structures exist in the water column [5]. The same obstacle is used here: a wall-mounted cubic cylinder of dimensions: $H \times 6H \times H$, hence its aspect ratio is A_R = Width / Length = 6. The cylinder represents an obstacle significantly higher than its neighbours, hence it is preceded by a natural boundary layer developing in the tank.

In order to characterize the flow downstream of the obstacle, 2D PIV (Particle Image Velocimetry) measurements are performed. PIV measurement planes are 500×1200 pix^2 with a spatial discretization of $11mm$. Acquisitions last $180s$, with an acquisition frequency of $15Hz$. Precisions on the PIV experimental set-up are available in [4] and the experimental error is estimated to be around 3% for the PIV velocity measurements.

In this study, a 3-bladed turbine model with $D = 725mm \simeq 3H$ diameter, recently developed at IFREMER [2], is used. The turbine model is equipped with 5-components blade root load-cells, measuring 2 forces and 3 moments for the 3 blades, in addition to torque and thrust transducers for the main rotation axis. Turbine parameters acquisition is in synchronisation with the PIV measurements, but with a sampling frequency of $120Hz$.

Both the obstacle and the turbine are at a scale of 1:20. Experiments are carried out for two Tip Speed Ratios (TSR): 0 (TSR0) and 4 (TSR4), with $TSR = \omega R/U_\infty$, $R = D/2$ the turbine radius and ω the rotation speed. $TSR = 4$ is the functioning point of the turbine, where the power extraction is maximal [6]. The in-line distance between the turbine and the wall-mounted obstacle is $16H$ (figure 3) and the far upstream velocity is $U_\infty = 1m/s$.

III – Vortices effects on Marine Current Turbine behaviour

Considering the first PIV results, as those presented on figure 4 showing large velocity fluctuations (u', w'), we propose to evaluate the best way to take into account the velocity time and spatial evolutions perceived by the turbine [3]. First, a vertical velocity profile is extracted as close as possible to the rotor ($x/D \simeq 0.2D$) and with a vertical size of $z = 1D$, along the red line on figure 4. This velocity profile is then spatially averaged and compared to a single point measurement, depicted by the green square on figure 4, at the same distance x of the rotor, but in the very centre of the turbine diameter. This second velocity measurement way is similar to what have been done in previous studies [1, 2], but with a closer distance between the velocity measurement point and the turbine; a too far distance being unfavourable to obtain a good coherence between incoming velocity variations and the turbine behaviour.

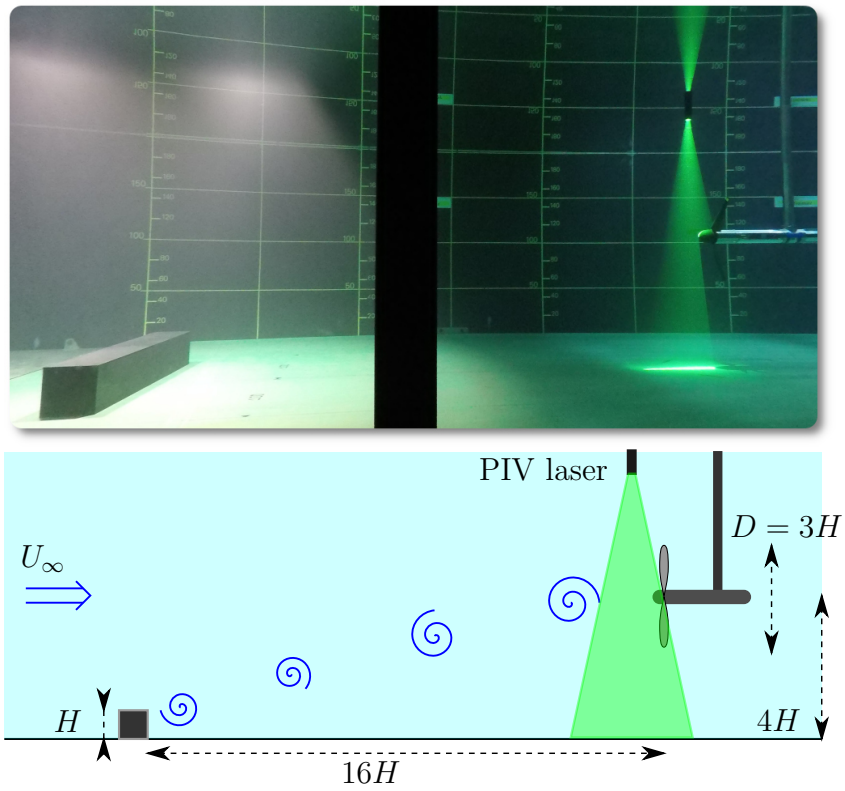

Figure 3 – Picture and schematic side view of the test set-up showing the obstacle, the experimental turbine and the PIV laser shooting

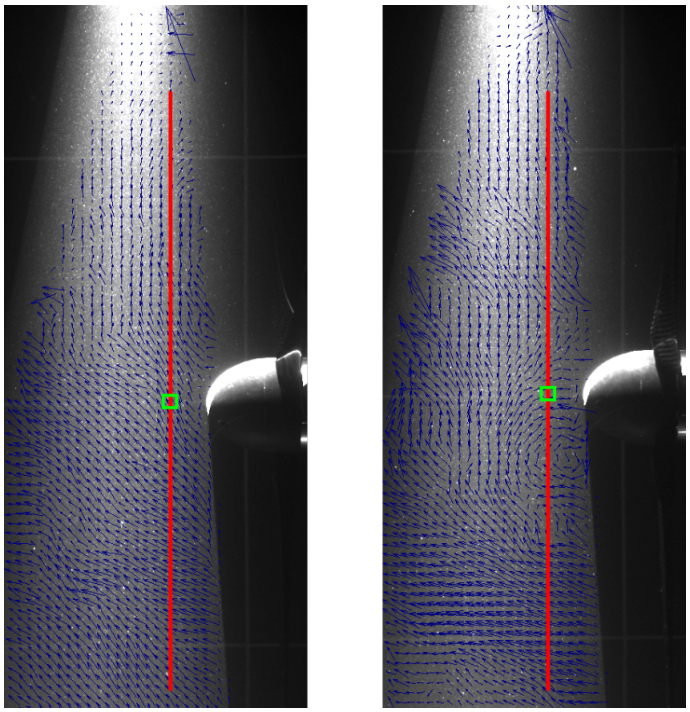

Figure 4 – Instantaneous fluctuating PIV field (u', w'), superimposed with a picture of the PIV laser shooting ahead of the turbine, at two different times and for $TSR = 4$. The red line and the green square stand for the profile and point respectively, where the velocity is extracted.

Both these signals are shown on figure 5 with u_{line} and u_{point} and on table 2 for time-average and standard-deviation values. The time-averaged values are slightly higher for TSR0 than for TSR4, because the turbine rotation induces a velocity deficit (blockage effect). Spatial averaging has a smoothing effect on the u_{line} signal comparing to u_{point}; standard-deviation is higher for u_{point}. However, the same large fluctuations are detected on the velocity signals, like for example at $t = 74s$ for TSR0 or $t = 97s$ for TSR4. The largest fluctuations are visible on the TSR4 plot and correspond to the field represented in figure 4. As expected, velocity fluctuations have a limited impact on the turbine parameters for TSR0, with a maximal thrust fluctuation of $\delta T = 20N$, but a considerably larger impact with a rotating turbine at TSR4 with thrust fluctuations up to $\delta T = 100N$.

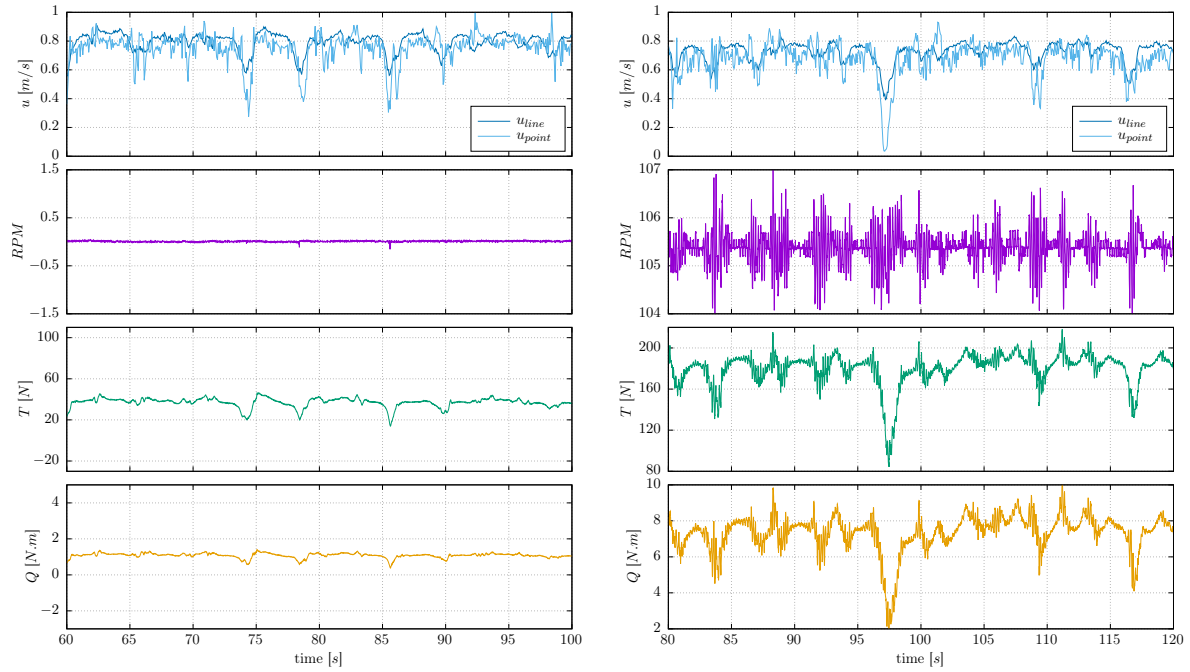

(a) $TSR = 0$ (b) $TSR = 4$

Figure 5 – Streamwise velocity signals (in a point at the altitude of the hub u_{point} and spatially averaged on a line u_{line}), the rotation speed RPM, the thrust T and the torque Q (top to bottom) for $TSR = 0$ and $TSR = 4$.

TSR	$\overline{u_{line}}$	$\sigma(u_{line})$	$\overline{u_{point}}$	$\sigma(u_{point})$
0	0.80	0.07	0.76	0.10
4	0.72	0.08	0.67	0.13

Table 2 – Time-averaged and standard-deviation of the velocities u_{line} and u_{point}, in m/s

Power Spectrum Densities (PSD) are plotted in figure 6 for the fluctuating part of each component of interest. The turbine signals have been down-sampled at the same acquisition frequency as the PIV : $f_s = 15Hz$. Streamwise velocity spectra are represented for both u_{line} and u_{point}, but the spectra slopes are different: it is steeper for u_{line} and closer to the other spectra, whereas the u_{point} PSD looks different for the highest frequencies. Except for u, the spectrum amplitude is generally more elevated for TSR4

than TSR0: fluctuations induced by the rotation are thus more elevated. All spectra show a classical decreasing slope, sign of turbulent dissipation in the flow (Richardson-Kolmogorov turbulence cascade), excepted for u_{point} and ω for TSR0. At TSR4, a peak at $3 \times f_r$, with $f_r = 1.76Hz$ the rotating frequency, is visible. This peak is absent of the u spectra, indicating that the turbine rotation speed does not affect the spectral content of the upstream flow.

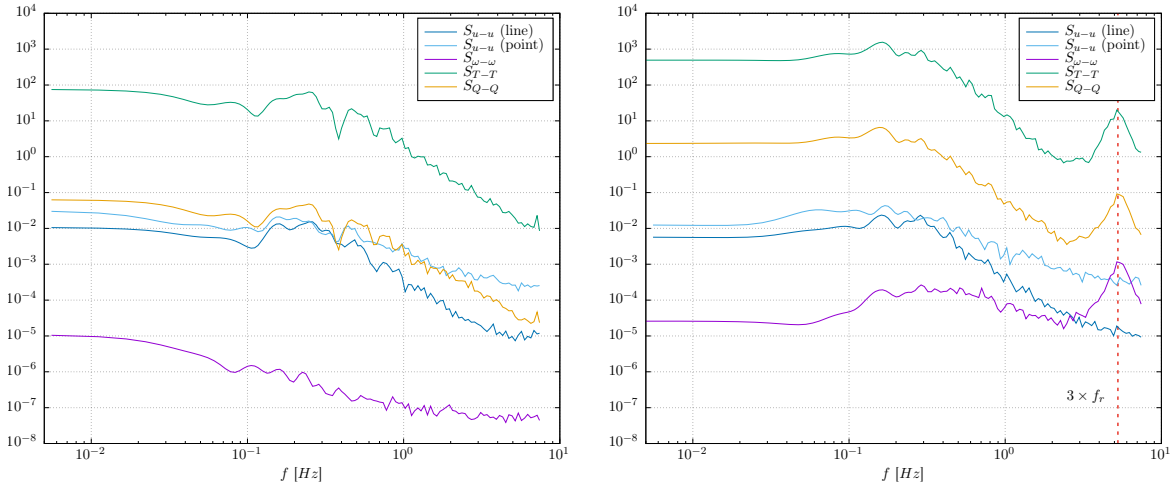

(a) $TSR = 0$ (b) $TSR = 4$

Figure 6 – Power Spectrum Densities for fluctuating components of streamwise velocity and turbine rotation speed, Thrust and Torque for $TSR = 0$ and $TSR = 4$.

Cross-Correlation ρ is evaluated between the upstream velocity and turbine loads for both TSR. ρ is first calculated for both u_{line} and u_{point}. Results have shown that the correlation peak is lower of 12% and 19% for TSR0 and TSR4 respectively, when ρ is computed with u_{point} compared to when ρ is computed with u_{line}. This is due to velocity fluctuations being considered along the turbine diameter for u_{line}, when u_{point} only takes into account the central point of the rotor. This reason, associated with the difference of the spectra slopes previously noticed, leads the authors to chose to evaluate ρ with u_{line} only. Results are illustrated in figure 7 and show a cross-correlation similar for T and Q. The ρ peak is higher when the turbine is rotating, indicating a better response of the turbine to external velocity fluctuations. Rotation velocity ω does not show a specific peak at TSR0, contrarily to TSR4 where a small peak ($\sim$ 0.1) is noticeable. Time lag t_l is evaluated at the peak position between the velocity and T (or Q): $t_l(\text{TSR0}) = -1/f_s = -0.07s$ and $t_l(\text{TSR4}) = -4/f_s = -0.27s$. These results are in agreement with the time-averaged velocities previously shown in table 2 : lower velocity values, thus higher time lag for TSR4. However, the relatively low sampling frequency prevents the time lag to be more accurate.

Signals are re-phased using the time lag t_l and the coherence is evaluated between u_{line} and the rotation speed, thrust and torque, for both TSR (figure 8). For all cases, no coherence at all is detected past $1Hz$, the turbine is acting as a low-pass filter with a cut-off frequency of $1Hz$. Same results were found in previous studies but the velocity measurements and the turbine were located further away from each other: at $4D$ [1] or $2D$ [2]. Hence, the low-pass filter effect of the turbine persists independently to the spacing. In a previous study [3], the idea has been emitted that this low-pass filter effect

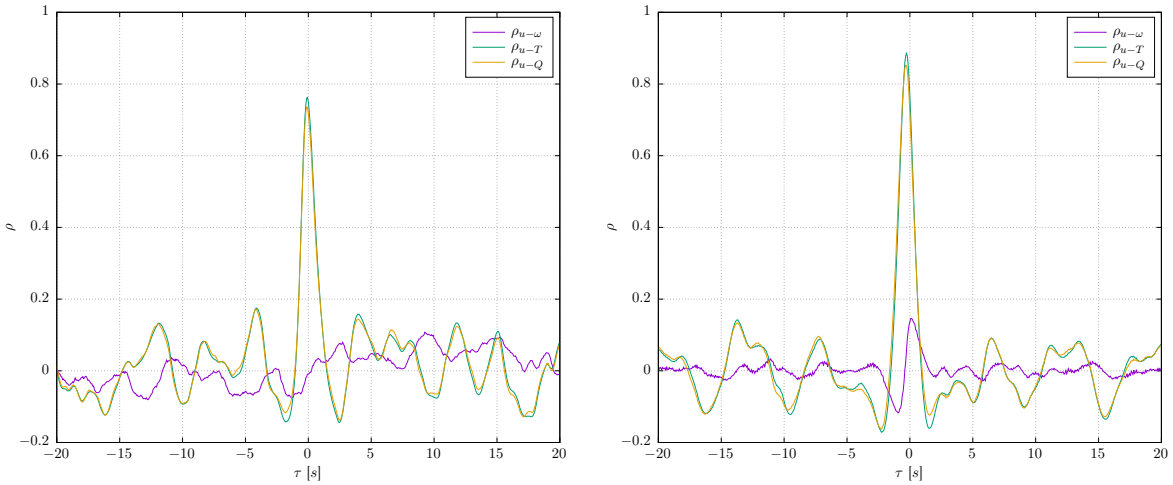

(a) $TSR = 0$ (b) $TSR = 4$

Figure 7 – Cross-Correlation ρ between the streamwise velocity u_{line} and the rotation speed ω, the Thrust T and the Torque Q for $TSR = 0$ and $TSR = 4$.

comes from the size of the turbine which acts as a spatial average and which prevents the smallest flow structures (with the highest frequencies) from being perceived. For low frequencies, results for TSR4 show good coherence (higher than 0.8) for both T and Q with a smooth decrease until $1Hz$. The coherence for the rotation speed ω is different however: the coherence is lower than 0.4 at low frequency, increases to $\simeq 0.9$ and then reduces at the cut-off frequency. The lower coherence for the lowest frequencies might be explained by the rotational speed control system, but this needs to be confirmed by further investigations. The result for TSR0, compared to TSR4, shows no coherence for all the frequencies, because the rotation speed is null.

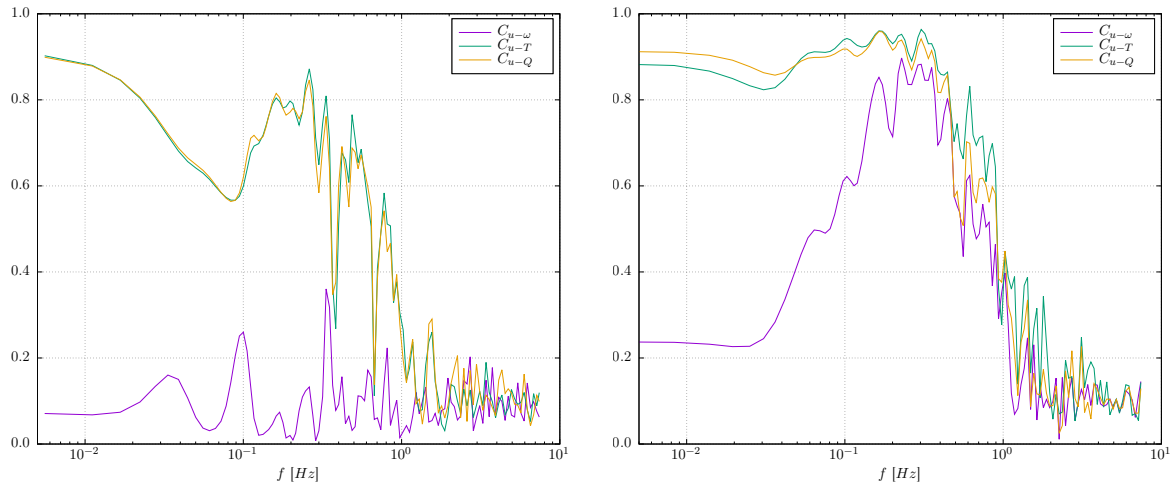

(a) $TSR = 0$ (b) $TSR = 4$

Figure 8 – Coherence between the streamwise velocity u_{line} and the rotation speed ω, the thrust T and the torque Q for $TSR = 0$ and $TSR = 4$.

IV – Conclusion & Perspectives

The presence of a wide wall-mounted obstacle in a flow causes large velocity fluctuations and some turbulent events, very persistent, rising up in the water column. The wake effect on an experimental turbine positioned at $16H$ downstream of the cylinder and at mid-height in the water column has been studied. To this aim, the turbine behaviour has been investigated with synchronous PIV measurements for $TSR = 0$ and $TSR = 4$.

The velocity used for comparison is a spatially averaged profile just upstream of the turbine. Results show that the signals of the rotating velocity ω, the thrust T and the torque Q follow the velocity fluctuations. A spectral analysis is lead and the spectra show a good adequacy between the flow fluctuations and the turbine response, excepted for the rotation speed. The rotating frequency is detected for ω, T and Q and is absent for the upstream velocity spectrum. Cross-correlation are plotted for all 3 metrics measured on the turbine and correlation goes up to 0.9 for T and Q for TSR4 and is lower (0.75) for TSR0: the turbine rotation may allow a better transcription of the flow velocity fluctuations. Time lag is larger for TSR4 than TSR0 due to the velocity deficit induced by the turbine rotation. The coherence between the upstream streamwise velocity and the rotation speed ω differs from those obtained with T and Q, especially for the lowest frequencies. This could be caused by the rotational speed control system, but further investigations are needed to confirm or not this point. The coherence shows the low-pass filter effect of the turbine for both TSR, it does not depend on the turbine rotation. This parameter is elevated for T and Q and more elevated for TSR4 than TSR0.

It has been previously shown that the incoming turbulence intensity of the flow has a strong impact on the turbine [6]. However, a flow with 15% of turbulence shall be compared to the present results with a incoming turbulence level of 1.5%, but with perturbations induced by an obstacle. The present study focuses on one position of the turbine. Additional measurements were performed at other positions downstream of the obstacle and analysis are ongoing.

Acknowledgement

The authors acknowledge the financial support of Ifremer and the Hauts de France Regional Council for the PhD studies. We are grateful to the French navy SHOM ("Service Hydrographique et Océanographique de la Marine") for providing access to bathymetric data (http://data.shom.fr/). We are most grateful to Thomas Bacchetti and Inès Belarbi for their assistance and precious advices.

References

[1] O. Durán Medina, F. G. Schmitt, R. Calif, G. Germain, and B. Gaurier. Turbulence analysis and multiscale correlations between synchronized flow velocity and marine turbine power production. *Renewable Energy*, 112:314 – 327, 2017.

[2] B. Gaurier, G. Germain, and J.-V. Facq. Experimental study of the Marine Current Turbine behaviour submitted to macro-particle impacts. In *Proceedings of the 12th European Wave and Tidal Energy Conference*, Cork, Ireland, 2017.

[3] B. Gaurier, G. Germain, and G. Pinon. How to correctly measure turbulent upstream flow for marine current turbine performance evaluation? In *Proceedings of the 3rd International Conference on Renewable Energies Offshore*, Lisbon, Portugal, 2018.

[4] M. Ikhennicheu, G. Germain, P. Druault, and B. Gaurier. Experimental analysis of the wake past wide wall-mounted obstacles. In *16èmes Journées de l'Hydrodynamique*, Marseille, France, 2018.

[5] M. Ikhennicheu, G. Germain, P. Druault, and B. Gaurier. Experimental study of coherent flow structures past a wall-mounted square cylinder. *Under review in Experiments in Fluids*, 2019.

[6] P. Mycek, B. Gaurier, G. Germain, G. Pinon, and E. Rivoalen. Experimental study of the turbulence intensity effects on marine current turbines behaviour. Part I: One single turbine. *Renewable Energy*, 66:729 – 746, 2014.

[7] P. Mycek, B. Gaurier, G. Germain, G. Pinon, and E. Rivoalen. Experimental study of the turbulence intensity effects on marine current turbines behaviour. Part II: Two interacting turbines. *Renewable Energy*, 68:876 – 892, 2014.

[8] SHOM. MNT Bathymétrique de façade Atlantique (Projet Homonim), 2015.

[9] J. Thomson, B. Polagye, V. Durgesh, and M. C. Richmond. Measurements of turbulence at two tidal energy sites in puget sound, WA. *IEEE Journal of Oceanic Engineering*, 37(3):363–374, 2012.